

Numerical Parametric Study of Geosynthetic-Gabion Walls under Different Surcharge Loads

Mahmoud Khalatbari ^a, Abolfazl Rezaeipour ^b, Rashid Hajivand Dastgerdi ^c, Mehran Ghannad^d, Sahand Shokri ^{e,*}

^aDepartment of Mining Engineering, University of Zanjan, Iran

^bAsfalt Tous Company, Tehran, Iran

^c Faculty of Civil Engineering and Resource Management, AGH UST, Poland

^d Faculty of Civil Engineering, University of Tehran, Tehran, Iran

^e Geotechnical Consultant, ParsOlang Consulting Engineers Co, Tehran, Iran

Received 07 October 2023, Accepted 18 October 2023

Abstract

The finite element procedures are extremely useful in gaining insights into the behavior of reinforced soil retaining walls. In this study, a validated finite element procedure was used with Abaqus for conducting a series of parametric studies on the performance of gabion facing wall with 2m vertical spacing Geo-grid under different surcharge loadings. The performance of the wall was presented with facing horizontal deformation along wall height, and compare to centrifuge model and field measurements. The soil properties include density, Young modulus, Poisson's ratio, and internal friction angle were among major variables of investigation. At low loading conditions, the impact of increasing density has a significantly greater effect on the deformation of the wall compared to high loads. As the loading increases, the effect of reducing the Young's modulus on deformations decreases. Moreover, with increasing loading, the effect of deformations due to the decrease in internal friction angle increases, but the rate of this increase decreases. The influence of Poisson's ratio on the deformation of the walls has decreased with increasing of loading. The results show that by the increase in load, even at a shallow depth, the applied stresses on the soil increase, leading to greater deformation of the soil above the wall, and the maximum magnitude is created at a higher elevation.

Keywords: Numerical Parametric Study, Geosynthetic-Gabion Wall, Surcharge Loads, Maximum Displacement

1. Introduction

A retaining wall is a structure built to hold back or retain soil and other materials, preventing them from eroding or collapsing. It is typically constructed in areas where there is a significant change in elevation or slope. Retaining walls are mainly provided in construction of roads, embankment, bridge abutments, basement in building, and have various types of facing reinforcement to enhance their stability and aesthetic appeal. A gabion retaining wall is a type of retaining wall that is constructed using wire mesh containers filled with rocks or other durable materials [1-4]. Gabion retaining walls provide stability by utilizing the weight and interlocking nature of the gabion units. The weight of the infilling materials within the baskets adds to the overall mass, enhancing resistance against earth

pressures and external forces. The placement and compaction of new soil layer during construction on previous layer would induce deformation in retaining wall [1-4]. The stress mobilization in the geosynthetic layers caused by different construction sequence of GRS-RWs, could lead to differences in the wall performance [1-4].

Allen and Bathurst (2002) underscored the need for a better understanding of the mechanical response of reinforced soil walls subjected to different loading conditions to develop more advanced design methodologies compared to the current limit equilibrium- based approaches, and it would lead to the development of an empirical-based design methodology (K-stiffness Method) [5]. They investigated the performance of reinforced soil walls using numerical models validated against physical

*Corresponding Author: Email Address: Sahandshokri@gmail.com

data gathered from field or laboratory models [6]. Hatami and Bathurst performed a comprehensive literature review on numerical simulations of reinforced soil walls, and it was determined that both the linear models proposed by Janbu (1963), or variants (Duncan et al, 1980), have been used in constitutive models for the backfill [7]. They have developed a numerical model and validated it by using quantitative measurements from three well-instrumented, large-scale test walls constructed and monitored in an indoor plane-strain facility [8].

Following their previous study, Hatami and Bathurst (2006) built four large-scale physical models of concrete segmental retaining walls with different arrangements of reinforced layers in RMC, and the numerical models made by FLAC software were validated with the measurements made on these physical models. They conducted a study to examine the impact of backfill compaction and the type of reinforcement on the response to end-of-construction and surcharge loading. The data they collected offers valuable insights for researchers looking to expand the existing repository of physical data related to response of reinforced soil walls [9-10].

Lei Xu at British Columbia University (2020), proposed a multi-stage constructed centrifuge modelling technique to simulate the construction sequence of GRS-RWs in the field. In addition, two series of finite element models were implemented to further study the wall performance [11]. Consequently, the multi-staged construction model showed better agreement with the field measurements.

The FEM analysis was applied to verify the results of centrifuge modelling studies. The dynamic result from FEM analysis showed that the studied gabion walls faced to a horizontal acceleration are stable up to 0.4 at the bottom area of the wall [11]. Parametric studies on reinforced soil behaviour have been reported for walls under construction and static loading (Seed et al. 1986; Kapurapu and Bathurst 1995, Ling et al. 1995, 2000; Rowe and Ho 1997; Bathurst et al. 2002, Ling and Leshchinsky 2003) [12-19].

In order to evaluate the influence of reinforcement layouts (length and spacing) on the wall performance, Ling et al, (2004) has analysed the full-scale reinforced soil retaining wall (6m) and the dynamic evaluation of centrifuge models [20]. Hoe I. Ling et al.(2005) conducted another parametric study on reinforced retaining walls, and the results indicated that soil properties, earthquake motions, and

reinforcement layouts (length and spacing) respectively in order of significance affected the EOC (end of construction) and after-shaking performance of the wall, while block interaction effect and cyclic properties of reinforcement were minimal [21].

In this research, a validated finite element procedure was used with ABAQUS for conducting a series of parametric studies on the performance of gabion facing wall with 2m vertical spacing Geo-grid under different surcharge loadings. The performance of the wall was presented with facing horizontal deformation along wall height, and compare to centrifuge model and field measurements. The major results of study are summarized and discussed.

2. Model Validation

In this study, Two-dimensional finite element model was created base on the centrifuge model developed by Lei Xu (2020) at British Columbia University [11]. The centrifuge model with 1/50 reduce scale of real structure, configuration of gabion block, reinforcement layouts and the location of monitoring instrumentation include strain gauge and earth pressure transducer is presented at Fig.1.

The foundation and backfill soil in centrifuge model is Nevada sand, which has 5% water content mixed with desirable compacted sand, 5 cm thickness for completing foundation, and constructed in three layers. In the centrifuge model, the gabions used in wall facing were made of a galvanized steel mesh filled with river stone, and the actual reinforcement in the model was simulated by using fiberglass mesh coated with polymeric film [11].

The base model for the validation, is a full-scaled test wall (at Izmir, Turkey) with 16 m height and gabion facing blocks, and two section of this wall with 1 m and 2m vertical spacing of Geo-grid were available to monitor the wall performance [11]. The reinforcements used are Tensar SR55 having secant modulus 600 KN/m at 5% strain, as reported by Ling et al (2000). The modular blocks used for the facing are 13 mm depth, 20 mm high and 40 mm wide, except the top and bottom blocks, which are 18 mm and 22 mm high [11].

There were different tests conducted on the model [11], but the reinforced retaining wall with 2m vertical spacing of Geo-grid and gabion facing was selected to analysis with numerical modelling through this article.

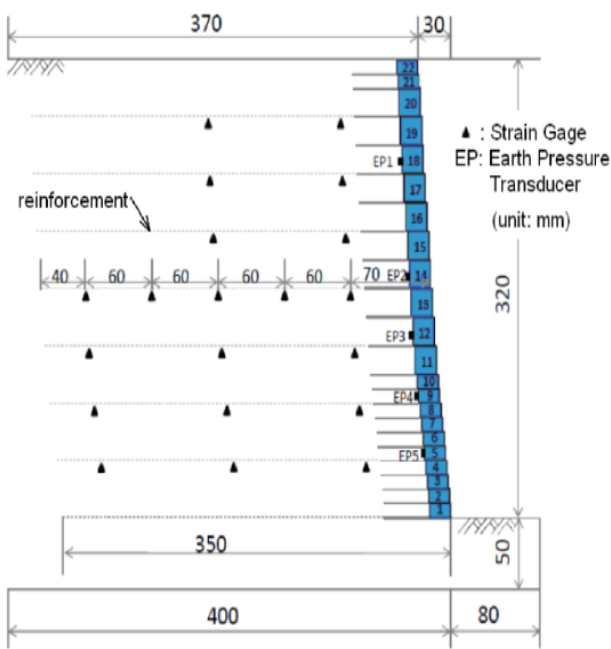


Fig. 1. Schematic view of Centrifuge model (2m vertical spacing) and instrumentations [3]

2.1. Numerical Modeling

The gabion-reinforced retaining wall is modelled using the two-dimensional (2D) plane strain finite element (FE) method. A plane-strain condition is considered in the analyses assuming that the strain in the direction perpendicular to the plane is zero. The retaining wall, characterized by a towering height of 16 meters, is meticulously founded upon a 2.5-meter-thick stratum of sandy foundation soil, ensuring the establishment of a secure structural base. The backfill material, integral to the wall's support system, comprises the specific geotechnical properties of Nevada sand soil. The facade of the wall presents a formidable configuration, consisting of gabion blocks, each spanning an impressive 20 meters in width and achieving a substantial height of 10 meters. These robust gabion blocks serve as the external cladding and load-bearing elements of the structure. To enhance the wall's stability and load-bearing capacity, a series of geogrid reinforcements is systematically inserted at regular 2-meter vertical intervals. This implementation commences when the wall attains a cumulative height equivalent to that of two stacked gabion blocks, which corresponds to 20 meters, culminating in the precise placement of 16 such geogrid layers at elevations meticulously tailored to the wall's structural requirements. Importantly, the geogrid reinforcements, measuring 17.5 meters in length, have been thoughtfully

designed to prevent any overhang or protrusion beyond the uppermost surfaces of the gabion blocks at any given elevation. Furthermore, the gabion blocks have been configured with a tail extending up to 2 meters from the rear face, aligning with best practices for optimal integration with the geogrid reinforcement. The judicious planning also ensures the absence of any gabion block tails within a designated 2-meter zone where geogrid reinforcement is employed, preserving the wall's structural integrity and uniformity.

In the numerical modelling approach, the backfill soil, the foundational soil layer, and the modular facing blocks have been meticulously represented using a 2D deformable continuum zone approach, effectively simulating their complex structural behaviours within the computational framework. The mesh size, critical for ensuring accurate and precise simulations, was determined through an extensive series of iterative analyses, considering various combinations of element numbers, ultimately resulting in a mesh configuration characterized by quadratic-shaped elements thoughtfully organized in a structural arrangement.

The reinforcements, pivotal for enhancing structural integrity and load-bearing capacity, have been systematically incorporated as 2D deformable wires featuring truss sections, reflecting their real-world performance characteristics. The thickness of the geogrids, a crucial element in the reinforcement system, has been specified at 0.0024 square meters, with their representation in the computational model achieved through the utilization of linear beam elements. Furthermore, the foundation soil, backfill, and facing components have been simulated using 4-node quadratic plane strain elements, ensuring a comprehensive and cohesive representation of their mechanical responses and interactions within the analytical framework.

The backfill soil employed in this analysis is characterized as granular Nevada sand, distinguished by an angle of internal friction measuring 41.2 degrees and a cohesion factor (C) of zero, with the computational representation of this backfill material being realized through the utilization of the Drucker-Prager constitutive model. The model parameters essential for describing the mechanical behaviour of the soil during the analysis are thoughtfully detailed and provided in Table 1, ensuring the accuracy and precision of the simulation. In a similar vein, the foundational substrate consists of medium dense sandy soil, and its behaviour is meticulously captured

within the computational framework using the unified sand model, further enriching the comprehensive characterization of the geotechnical system under investigation. The density, modulus of elasticity and poisson's ration are presented in Table 1:

Table1:
The modeling properties of Soil [11]

Model Parameters	Units	Value
Mass Density (ρ)	kg/m ³	1600
Elastic Modulus (E)	MPa	20.7
Poisson's ratio (ν)	-	0.42
Friction Angle (ϕ)	(°)	41.2
Dilation Angle (Ψ)	(°)	4

The backfill and foundation soils were expressed using Drucker-Prager model. Performance of Drucker-Prager model for non-cohesive granular material is better than Mohr-Coulomb criterion. For plain strain condition, the Mohr-Coulomb parameters can be converted to Drucker-Prager parameters as follows [22]:

$$\tan\beta = \frac{3\sqrt{3}\tan\phi'}{\sqrt{9+12\tan^2\phi'}} \text{ for } \phi' = 41.2^\circ \rightarrow \beta = 46.3^\circ \quad (1)$$

$$d = \frac{3\sqrt{3}c'}{\sqrt{9+12\tan^2\phi'}} \text{ for } c' = 0 \rightarrow d = 0 \quad (2)$$

Where the parameter β represents the angle of friction, which is transformed = 46.3° , d indicates cohesion for Drucker-Prager yield criterion. In the analysis, the cohesion of granular sand is zero, so the value of parameter d is equal to zero.

In order to provide distinct interaction characteristics to various sections of the retaining wall, interface properties were segregated. Moreover, an automated general contact boundary surface was applied to the entire model to ensure consistent contact definition for all undefined surface-based interactions. This specific interaction property was primarily designated for the interface between individual blocks. The "surface pair" option, denoted as "all with self," was chosen to encompass all exterior surfaces and angular features. For the block-block interaction, both normal and tangential parameters were established. In the context of mechanical behaviour in the normal direction, "hard contact" was configured for pressure overclosure, allowing for separation after initial contact. The shear resistance of the block-block interface was represented in ABAQUS using the

Coulomb friction model with a designated friction coefficient as given by:

$$\tau = \mu_s \sigma_N \quad (3)$$

Where τ is the shear stress, σ_N is the normal stress and μ_s is the coefficient of static friction. In addition to implementing a general contact interaction, specific individual contact interactions were integrated into the modelling process. For the interfaces between soil and individual blocks, individual contact pairs based on surface interactions were introduced. At the tangential behaviour, the friction formulation base on penalty was used for both block-soil and block-block interface with friction coefficient $\mu = 0.7$.

The contact pair interaction requires the explicit specification of master and slave surfaces. Accurate identification of the master and slave surfaces is imperative for achieving a precise contact surface simulation. Typically, the master surface is determined to be the denser or stronger of the two surfaces when they come into contact, with the other surface designated as the slave. Consequently, in the context of the block-soil interaction scenario, the soil serves as the slave surface, while the facing block acts as the master surface. To ensure the binding of soil nodes to reinforcement nodes, a "Tie constraint" was employed. This approach assumes minimal slippage between the geogrid and the soil, attributed to the significant difference in aperture sizes between the geogrid and the soil layers, as observed in Huabei et al. (2009). The reinforcement is securely affixed to the gabion facing block, and this connection can be more accurately modelled by utilizing the coupling constraint option in ABAQUS. Surface-based coupling constraints establish rigid connections between a reference node (reinforcement) and nodes located on a surface (gabion facing block).

A system comprised of various components was assembled to establish interactions among these components, and boundary conditions were defined. At the far back end of the wall, a roller connection was implemented. These connections are constrained from moving horizontally but are allowed vertical movement. To accurately replicate real-world conditions that may exist in the field, a foundation soil layer of a specific height was assumed. This allows for the introduction of a geostatic step, facilitating the inclusion of existing soil pressure, and ensures that the foundation soil is in equilibrium with no displacement. The foundation interface, specifically

the lower portion of the foundation soil, was modelled to prevent movement in both horizontal and vertical directions.

Interactions were established between the facing of the wall, the backfill soil, and the reinforcement elements. The wall's construction was simulated to mimic the natural process observed in the field. Consequently, the wall was constructed in distinct lifts, accounting for its actual behaviour, and each lift was placed after completion. A single lift was defined within a specific analysis step, and gravitational loads were applied to the soil, facing blocks, and reinforcement elements in that lift set. This process was repeated for each step, ensuring convergence towards a solution.

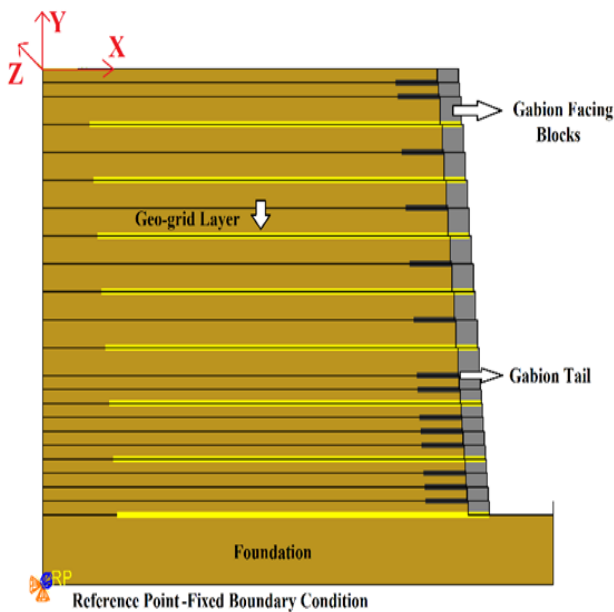


Fig. 2. The Retaining wall with reference point and fixed boundary condition in Abaqus

Primary reinforcement layers were simulated as embedded regions within backfill soil and gabions. The embedded element technique in Abaqus is used to simulate a group of elements (reinforcement) embedded in "host" elements (soil). The secondary reinforcement (gabion tail) layers were also simulated as embedded regions within the backfill but tied to the gabions.

In ABAQUS, the mesh is usually created locally for each part (e.g., each reinforcement layer and gabion block); thus, linear-elastic shell elements were selected for soil body and gabion blocks to make sure the number of nodes is consistent on all interface of two parts. The linear beam element was used for both primary and secondary reinforcement. The properties

of gabions, primary and secondary reinforcement are presented in table 2, 3 respectively [11].

Table2: Material properties of gabions [11]

Density Value	2000 Kg/m ³
Elastic, Poisson's Ratio	2000 kPa, 0.3
Mohr Coulomb Plasticity	Friction Angle=45°, Cohesion=560 kPa

Table3: Properties of primary and secondary reinforcement [11]

Parameters	Geo-grid	Gabion Tail
Length (m)	17.5	2
Thickness (cm)	0.24	0.27
Young's modulus (MPa)	2600	3700
Poisson's Ratio	0.1	0.1
Equivalent Stiffness (kN/m)	6240	9990
Tensile Strength (KN/m)	412	60

As it is shown on Fig.3, the results of numerical modelling for lateral displacements are between the range of centrifuge models and field measurements, and shows good agreement with them. Consequently, the results of numerical modelling for both Lei Xu and current study have a close relation.

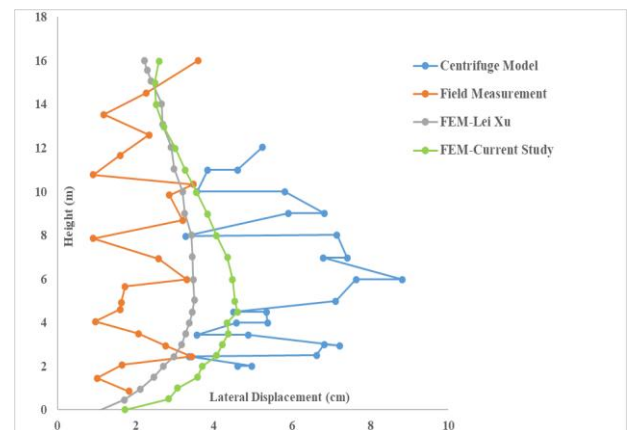


Fig. 3. The simulated and measured fall facing horizontal displacement of 2m spacing Geo-grid

2.2. Parametric Study

The effect of soil properties on the wall performance are investigated based on lateral deformation on wall face under different loading conditions. The different soil parameters and the value of loading are presented in table 4. Determining the more significant parameters on the horizontal deformation of the wall

under different surcharge loads are the main goal of this section.

Table 4:
The parametric study of soil properties under different loading

Parameters	Unit	Loading Value (kPa)
		No load, 20, 80, 120
ρ (Mass Density)	(kg/m ³)	14,16,18
ν (Poisson's ratio)		0.35, 0.42, 0.45
Es (Elastic Modulus)	(Mpa)	10, 20.7, 30
ϕ (Friction Angle)	(°)	35, 41.2, 46

As it is mentioned in previous section, the cohesion is zero for granular sand, and the value of friction angle in Mohr-Coulomb criterion can be transformed to the parameter β in the Drucker-Prager criterion. Therefore, the parameter β for three different value 32, 41.2 and 46 is equal to 43.3, 46.8 and 49 respectively. Table 5-8 presents the maximum displacement of wall facing achieved by changing parameters density, elastic modulus, friction angle, and Poisson's ratio respectively. In addition, column Diff evaluate the raising of deformation between lower and upper limits of four mention parameters, and Diff% column presents the growth percentage of deformation results.

Table 5:
Sensitivity analysis of wall deformation toward density and load changes

	14 (Kg/m ³)	16 (kg/m ³)	18 (kg/m ³)	Diff	Diff %
No Load	0.0418611	0.046067	0.050531	0.00867	+20.7
20 kPa	0.0545033	0.061627	0.068836	0.014332	+26.2
80 kPa	0.0768638	0.083715	0.090485	0.013621	+17.7
120 kPa	0.0929091	0.099265	0.105534	0.012625	+13.5

Table 6:
Sensitivity analysis of wall deformation toward Elastic modulus and load changes

	30 MPa	20.7 MPa	10 MPa	Diff	Diff %
No Load	0.036059	0.046067	0.070754	0.034695	+96.2
20 kPa	0.047755	0.061627	0.106875	0.05912	+123.7
80 kPa	0.067724	0.083715	0.135411	0.067687	+99.9
120 kPa	0.081671	0.099265	0.155767	0.074097	+90.7

Table 7:
Sensitivity analysis of wall deformation toward friction angle and load changes

	46 (°)	41.2 (°)	35 (°)	Diff	Diff %
No Load	0.04616	0.046067	0.046804	0.000644	+1.4
20 kPa	0.059906	0.061627	0.065933	0.006028	+10.1
80 kPa	0.079967	0.083715	0.092554	0.012587	+15.7
120 kPa	0.093947	0.099265	0.110692	0.016745	+17.8

Table 8:
Sensitivity analysis of wall deformation toward Poisson's ratio and load changes

	0.35	0.42	0.45	Diff	Diff %
No Load	0.03546	0.046067	0.052165	0.016705	+47.1
20 kPa	0.051864	0.061627	0.067835	0.015971	+30.8
80 kPa	0.073519	0.083715	0.090526	0.017007	+23.1
120 kPa	0.088608	0.099265	0.106469	0.017861	+20.1

Under higher loading conditions, the increase in soil density leads to a comparatively reduced stress variation when juxtaposed with the applied load, resulting in diminished deformations in the retaining wall. Consequently, in situations characterized by low loading, the influence of augmented density exerts a considerably more substantial impact on wall deformation than in high-load scenarios. As the applied load escalates, the diminishing effect of reducing the Young's modulus on deformations becomes apparent. Additionally, as loading intensifies, the impact of deformations attributed to a reduction in the internal friction angle increases, albeit at a diminishing rate. Concurrently, the influence of Poisson's ratio on wall deformation diminishes with increasing load. Horizontal displacement contours of the retaining wall are depicted in Figure 4, while Figure 5 illustrates the horizontal displacement concerning wall height. Clearly, it is observable that elevating surcharge loads extends the maximum displacement contours towards the upper segment of the wall facing, generally resulting in amplified horizontal displacements. The increase in stress with depth during the unloaded state and the accompanying horizontal expansion, which is governed by the designated Poisson's ratio, induce the maximum displacement to transpire marginally higher within the bottom segment where the wall is under constraint. Under elevated loading, even within shallower depths, the applied stresses on the soil surge, thereby provoking more pronounced deformations in the soil situated above the wall.

Although the most substantial stresses originate at the base of the wall, these dual conditions collectively foster heightened wall displacement at an elevated altitude, resulting in the emergence of the maximum magnitude at a higher elevation.

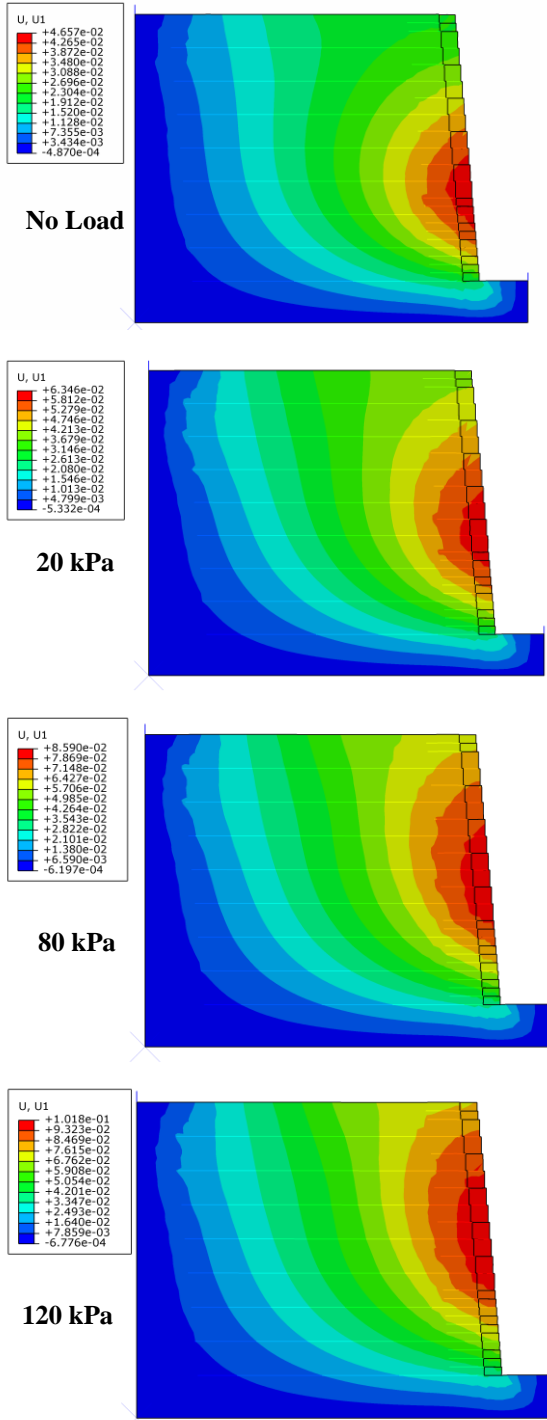


Fig. 4. Horizontal displacement contours under different loading condition

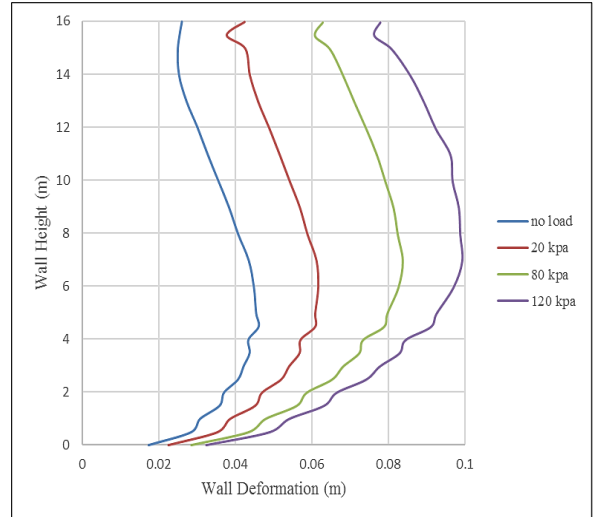


Fig. 5. Wall deformation under different loading conditions

3. Conclusion

A validated finite element procedure was used to conduct a series of parametric studies related to the surcharge loading behaviour of geosynthetic-reinforced soil retaining walls. The following conclusions were drawn based on the results of parametric studies:

- The horizontal displacement of the wall exhibits a direct correlation with the surcharge load, demonstrating an increase as the load magnitude rises.

- Density changes have a greater impact on wall deformation during lower surcharge loads. As the surcharge load increases from zero to 120kPa, the influence of density on wall horizontal deformation decreases from 20.7% to 13.5%.

- With the increase in surcharge load, the effect of reducing Young’s modulus on deformation diminishes.

- Our study reveals that reducing the Young’s modulus from 30 MPa to 10 MPa under no surcharge load leads to a 96.2% increase in wall deformation. However, this increase is reduced by 6% when the surcharge load intensifies from zero to 120kPa.

- The effect of decreasing the internal friction angle on the horizontal wall displacement increases from 1.4% to 18% as the surcharge load goes from zero to 120kPa.

- As the surcharge loads increase from zero to 120kPa, the influence of increasing Poisson’s ratio on the horizontal deformation of the wall decreases from 47% to 20%.

- Among the all four parameters, the internal friction angle has the least impact on wall displacements, while Young’s modulus has the most significant effect.

References

- [1] Product data sheet of Metal Gabion of Garware-Wall Ropes Ltd. Geosynthetics Division.
- [2] IS Code 280, Steel wire for general engineering purposes, 2006.
- [3] Su Yang, Amin Chegnizadeh, Hamid Nikraz (2013). Review of Studies on Retaining Wall's Behavior on Dynamic/Seismic Condition, *Journal of Engineering Research and Applications*, 3 (6),1012-1021.
- [4] Anderson, D. G. N. C. H. R. P. N. R. C. T. R. B. A. A. o. S. H. and O. Transportation (2008). Seismic analysis and design of retaining walls, buried structures, slopes, and embankments. Washington, D.C., Transportation Research Board.
- [5] Bathurst, R.J., Walters, D.L., Esfehiani, M., El-Emam, M. and Blatz, J.A. (2002b) Physical modelling of geosynthetic walls and embankments (Invited keynote paper), Proc. of International Conference on Physical Modeling in Geotechnics, (ICPMG), St. Johns, Newfoundland, 10-12 July 2002, pp. 21-30.
- [6] Bathurst, R.J., Walters, D., Hatami, K. and Allen, T.M. (2001) Full-scale performance testing and numerical Modelling of reinforced soil retaining walls (Invited keynote paper), Proc. of International Symposium: Landmarks in Earth Reinforcement, IS Kyushu 2001, 14- 16 November 2001, 26 p.
- [7] Bathurst, R. J., and Hatami, K. (2001). Review of numerical modeling of geosynthetic reinforced soil walls. Proc., 10th Int. Conf. on Computer Methods and Advances in Geomechanics, 1223–1232.
- [8] Hatami, K., and Bathurst, R. J. (2005). Development and verification of a numerical model for the analysis of geosynthetic reinforced-soil segmental walls. *Can. Geotech. J.*, 42(4), 1066–1085.
- [9] Hatami.k, Bathurst.R.J (2006). Numerical Model for Reinforced Soil Segmental Walls under Surcharge Loading. *Journal of Geotechnical and Geoenvironmental Engineering*, 132 (6), 673-684.
- [10] Bathurst, R.J. (2007). REINFORCED SOIL RETAINING WALL TESTING, MODELING AND DESIGN. IGC. 14-16.
- [11] Lei Xu, (2020). Centrifuge Modeling and Numerical Analysis of Geosynthetic- Reinforced Soil Retaining Walls Having Different Facings, Doctoral Dissertation, Columbia University, Graduate school of art and science.
- [12] Seed, R. B., Collin, J. G., and Mitchell, J. K. (1986). FEM analyses of compacted reinforced soil walls. Proc., Second Symp. on Numerical Models in Geomechanics, Balkema, Rotterdam, The Netherlands, 553–562.
- [13] Kapurapu, R., and Bathurst, R. J. (1995). Behavior of geosynthetic reinforced soil retaining walls using the finite element methods. *Computers and Geotechnics*, 17, 279–299.
- [14] Ling, H. I., Tatsuoka, F., and Tateyama, M. (1995). Simulating performance of GRS-RW by finite element procedure. *J. Geotech. Eng.*, 121(4), 330–340.
- [15] Ling, H. I., Cardany, C., Sun, L.-X., and Hashimoto, H. (2000). Finite element analysis of a geosynthetic-reinforced soil retaining wall with concrete-block facing. *Geosynthet. Int.*, 7(3), 163–188.
- [16] Rowe, R. K., and Ho, S. K. (1997). Continuous panel reinforced soil walls on rigid foundations. *J. Geotech. Geoenviron. Eng.*, 123(10), 912–920.
- [17] Bathurst, R. J., Hatami, K., and Alfaro, M. C. (2002). Geosynthetic reinforced-soil walls and slopes: Seismic aspects. *Geosynthetics and their Applications*, S. K. Shukla, ed., Thomas Telford, London, 327–392.
- [18] Bathurst, R. J., Walters, D. L., Hatami, K. , Saunders, D. D., Vlachopoulos, N. , and Burgess, G. P. (2002). Performance testing and numerical modeling of reinforced soil retaining walls. Proc. Seventh International Conference on Geosynthetics, Ph. Delmas, J. P. Gourc, and H. Giard, eds., Swets and Zeitlinger, Lisse, The Netherlands 217–220.
- [19] Ling, H. I., and Leshchinsky, D. (2003). Parametric studies of the behavior of segmental block reinforced soil retaining walls. *Geosynthet. Int.*, 10(3), 77–94.
- [20] Ling, H. I., Liu, H., Kaliakin, V., and Leshchinsky, D. (2004). Analyzing dynamic behavior of geosynthetic-reinforced soil retaining walls. *J. Eng. Mech.*, 130(8), 911–920.
- [21] Hoe I. Ling, Huabei Liu; Yoshiyuki Mohri, (2005). Parametric Studies on the Behavior of Reinforced Soil Retaining Walls under Earthquake Loading, 10.1061/(ASCE)0733-9399(2005)131:10(1056), *Journal of Engineering Mechanics*.
- [22] Sam Helwany, “Lateral earth pressure and retaining walls,” in *Applied soil mechanics with ABAQUS applications*, (John Wiley, Canada,2007), pp. 233-286.